

Butyrate selectively targets super-enhancers and transcriptional networks associated with human mast cell function

Jelle Folkerts^{1,2}, Marjolein J. W. de Bruijn¹, Wilfred F.J. van IJcken³, Rudi W. Hendriks¹ and Ralph Stadhouders^{1#}

¹*Department of Pulmonary Medicine, Erasmus MC, Erasmus University Medical Center Rotterdam, The Netherlands*

²*Department of Pathology, Stanford University School of Medicine, Stanford, USA*

³*Center for Biomix, Erasmus MC, Erasmus University Medical Center Rotterdam, The Netherlands*

[#]*Corresponding author*

Corresponding author:

Ralph Stadhouders, PhD,
Erasmus MC, University Medical Center Rotterdam
Dept. of Pulmonary Medicine
Room Ee2251a, 3000 CA Rotterdam, The Netherlands
Phone: +31-107043697
Email: r.stadhouders@erasmusmc.nl

Short title: Butyrate Targets Mast Cell Super-Enhancers

Keywords: Acetylation, Butyrate, Histone deacetylase, Mast cells, Super-enhancers

Abstract

Mast cells are key drivers of allergic inflammation. We have previously shown that butyrate, a short-chain fatty acid derived from dietary fibers, inhibits human mast cell activation and degranulation. Here, we characterized the mechanisms underlying butyrate-mediated control of mast cell activity. To this end, we assessed the genome-wide impact of butyrate, a histone deacetylase (HDAC) inhibitor, on the epigenomic control of mast cell gene expression by integrating transcriptome and histone acetylation (H3K27Ac) profiles obtained from butyrate-treated primary human mast cells. Butyrate affected a selective set of genes and gene regulatory elements in mast cells. Most prominent was the hypo-acetylation of promoter regions of highly expressed genes and super-enhancers controlling key mast cell identity genes. Perturbation of super-enhancer activity via pharmacological bromodomain inhibition suppressed degranulation of primary human mast cells, evoking a repression of key mast cell identity genes that resembled the inhibitory effects of butyrate. Our data indicate that butyrate inhibits human mast cell activity via a surprisingly selective targeting of super-enhancers to regulate the core mast cell transcriptional program.

Abbreviations

ChIP-Seq:	Chromatin Immunoprecipitation coupled to high-throughput Sequencing
HAT:	Histone-acetyltransferase
HDAC:	Histone deacetylase
HDACi:	Histone deacetylase inhibitor
Mb:	Megabase
MC:	Mast cell
PBMC:	Peripheral blood mononuclear cell-derived human mast cell
RNA-seq:	RNA sequencing
SCFA:	Short-chain fatty acid
SE:	Super-enhancer
SP:	Substance P
TE:	Typical-enhancer
TSS:	Transcription Start Site
RPKM:	Reads Per Kilobase per Million

Conflicts of interest relevant to this work

The authors have declared that no conflict of interest exists.

Introduction

Mast cells are major effector cells of the immune system. They reside in virtually all vascularized tissues, especially those in direct contact with the external environment. Mast cells mediate IgE-associated type 2 immune responses, which have been implicated in anti-parasite immunity but also allergies, asthma, chronic rhinosinusitis with nasal polyps, and urticaria¹⁻⁶. Allergens can crosslink allergen-specific IgE bound to the high-affinity IgE receptor (FcεRI) on the mast cell surface, resulting in their degranulation¹. This causes the immediate release of preformed granule mediators such as histamine, heparin, and certain proteases, followed by *de novo* synthesis and release of various lipid mediators and cytokines. More recently, the Mas-related G protein-coupled receptor X2 (MRGPRX2) expressed on mast cells was shown to participate in IgE-independent mast cell activation, resulting in drug-induced pseudo-allergic reactions (e.g. against antibiotics)⁷⁻⁹.

Mast cell maturation, phenotype and function are determined by gene expression programs controlled by endogenous and microenvironmental factors¹⁰. These include the microbiome, which directly contributes to the development and maturation of the immune system¹¹. Short chain fatty acids (SCFAs) including butyrate, propionate and acetate - derived from bacterial fermentation of dietary fibers - are considered key metabolites in the regulation of host physiology and pathophysiology¹²⁻¹⁴. Butyrate critically affects differentiation and function of many lymphocyte populations as well as myeloid cells such as macrophages and dendritic cells¹⁵⁻²³.

SCFAs, particularly butyrate, were shown to promote gut homeostasis and immunity via control of histone acetylation and subsequently gene transcription^{24,25}. The acetylation state of a given genomic locus is controlled by two classes of antagonistic histone modifying enzymes, histone acetyl transferases (HATs) and histone deacetylases (HDACs), which add and remove target histone acetyl groups, respectively. Histone acetylation is a hallmark of active promoter regions and transcription start sites (TSSs), but also occurs at distal gene regulatory elements such as enhancers^{26,27}. Particularly high levels of histone acetylation are located at super-enhancers, a class of powerful enhancers that control the expression of key cell type-specific genes²⁸. Butyrate is a known inhibitor of all class I/II HDACs^{29,30} and can significantly affect gene expression, since histone acetylation is generally associated with accessible chromatin and active gene transcription^{31,32}. HDAC inhibition is thus expected to trigger histone hyperacetylation and facilitate transcriptional activation. However, whether butyrate affects histone acetylation status and the gene regulatory function of super-enhancers remains largely unknown.

We recently reported that butyrate inhibits human mast cell activation and degranulation, which was associated with reduced expression of genes critical for FcεRI-mediated signaling - likely via epigenetic mechanisms³³. How butyrate exerts such specific effects on gene expression in mast cells while targeting a very basal component

of transcriptional regulation remains incompletely understood. To address this question, we integrated transcriptome and longitudinal profiling of histone acetylation measurements to identify molecular mechanisms underlying selective gene expression changes in primary human mast cells exposed to butyrate – ultimately resulting in potent mast cell inhibition.

Results

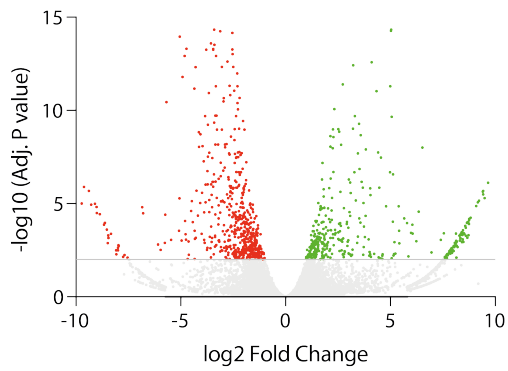
Butyrate selectively regulates gene transcription in primary human mast cells

To characterize the impact of butyrate exposure on the mast cell transcriptome, we measured gene expression profiles of two independent primary human mast cell cultures upon 24 h of 5mM butyrate treatment using RNA-Sequencing (RNA-Seq). Across all genes detected, 551 were upregulated by butyrate whereas 864 genes were downregulated (FDR<0.05; **Fig. 1A,B**). Correlation of gene expression values between the two biological replicates was high, both before and after butyrate treatment ($R^2>0.97$, **Supplementary Fig. 1A,B**). Pathway enrichment analyses indicated that downregulated genes were mainly associated with leukocyte and mast cell activation (**Fig. 1C,D**, upper panels). Indeed, expression of genes coding for proteins involved in FcεRI- and MRGPRX2-mediated mast cell activation was significantly downregulated (including BTK, SYK, LAT and MRGPRX2, **Supplementary Table 1**), supporting our earlier findings that butyrate inhibits mast cell activation induced via IgE and substance P (an MRGPRX2 ligand). Upregulated genes were enriched in more diverse biological pathways (**Fig. 1C,D**, lower panels), including genes involved in responses to metal ions (i.e., MT1 family proteins), cellular responses to external stimuli and Ras/Rab GTPase signaling (**Fig. 1C,D**, lower panels, **Supplementary Table 1**).

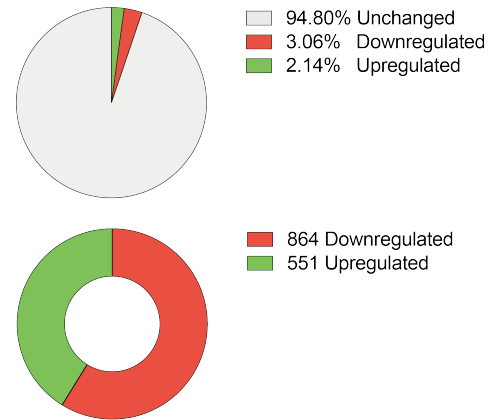
The downregulated genes - in particular canonical mast cell genes - showed substantially higher median basal expression values than unaffected or upregulated genes (**Fig. 1E**). This is in line with a previous study in cancer cells demonstrating that HDAC inhibitors are more likely to repress highly expressed genes²⁶. Conversely, upregulated genes displayed slightly lower basal expression levels as compared to unaffected genes (**Fig. 1E**). Nevertheless, high basal expression levels were not solely predictive for responsiveness to butyrate treatment, as the 50 most highly expressed genes did not respond to butyrate treatment (**Fig. 1F**).

Together, these results show that butyrate, in primary human mast cells, selectively downregulates gene expression associated with leukocyte/mast cell activation and upregulates a more diverse group of genes. Basal expression levels alone only partially predict responsiveness to butyrate treatment, indicating a more selective mechanism of action through which butyrate exerts its effects.

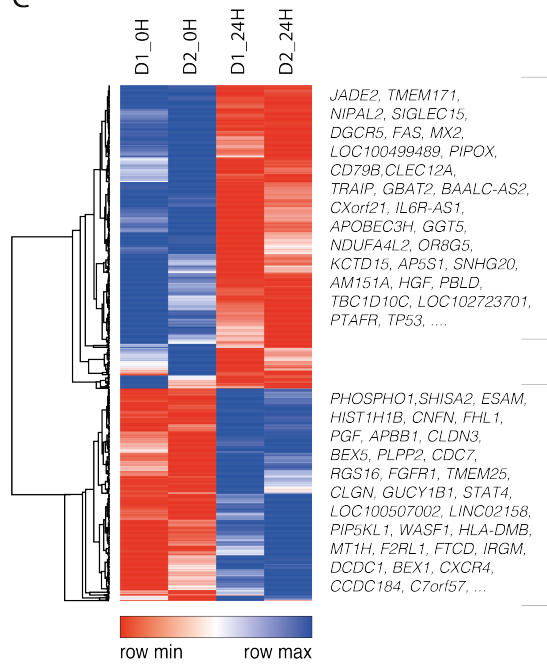
A



B

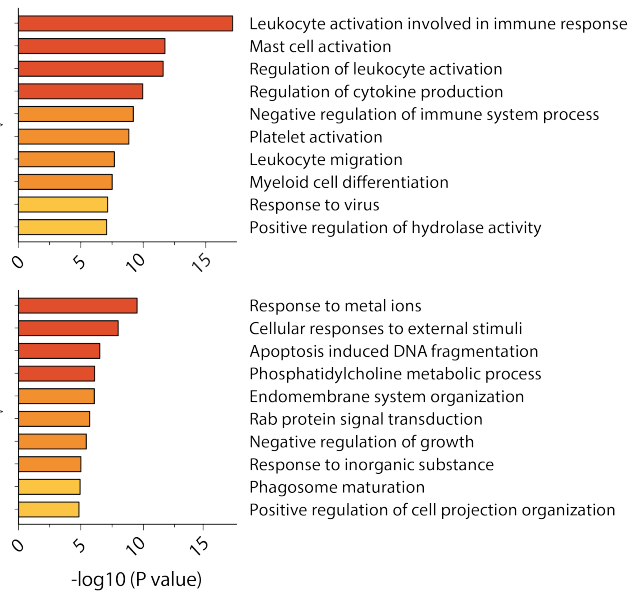


C

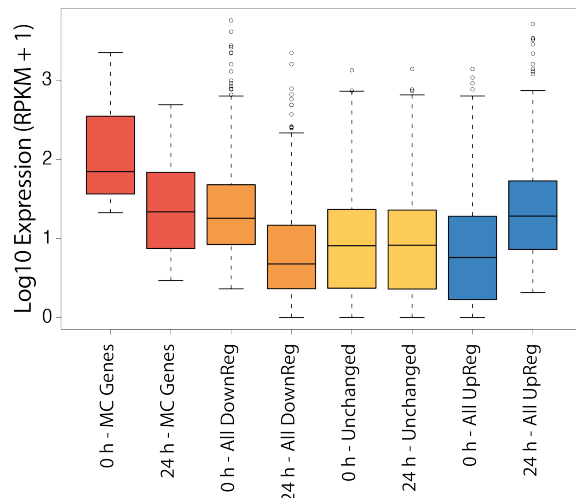


D

Pathway Enrichment Analysis



E



F

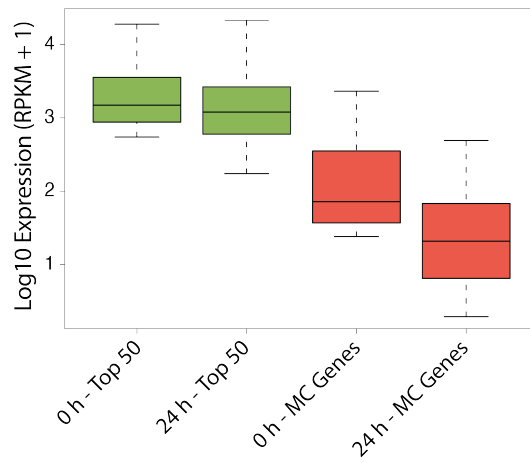


Figure 1. Butyrate selectively downregulates gene expression associated with leukocyte/mast cell activation. Gene expression profiles of primary human mast cells after 24 h of 5mM butyrate treatment was measured using RNA-Sequencing (RNA-Seq; two biological replicates from independent donors). **(A)** Scatter plot of downregulated (indicated in red), upregulated (indicated in green) and unchanged genes (indicated in grey) in response to 24 h butyrate treatment. **(B)** Proportions (*top*) and absolute numbers (*bottom*) of downregulated (red), upregulated (green) and unchanged genes (gray). **(C)** Heatmap showing scaled expression levels of down- and upregulated genes, selected example genes (with the highest fold change) are presented next to the heatmap. **(D)** Pathway enrichment analysis of downregulated (top) and upregulated (below) genes. **(E)** Expression changes in response to butyrate of canonical mast cell genes (red), downregulated genes (orange), unchanged genes (yellow), upregulated genes (blue). **(F)** Expression changes in response to butyrate of the top 50 highest expressed genes (green) and canonical mast cell genes (red). MC, mast cell; RPKM, reads per kilobase per million

Butyrate triggers global histone hyperacetylation

To map the epigenomic landscape of two primary human mast cell cultures, D1 and D2, after butyrate treatment, we performed ChIP-Seq specific for histone 3 lysine 27 acetylation (H3K27Ac) and histone 3 lysine 4 dimethylation (H3K4Me2) after 0, 3, 12 and 24 h of butyrate treatment. H3K27Ac is a well-characterized acetylation mark that strongly correlates with transcriptional activity; H3K4Me2 is also associated with active genes yet is not an HDAC target³⁴. Genome-wide H3K27Ac coverage was markedly increased by butyrate (up to ~2.6 fold), which was already apparent after 3 h and remained elevated after 24 h of treatment (**Fig. 2A**, left panel). The relative increase in H3K27Ac+ regions across the genome was essentially independent of enrichment calling parameter settings (**Supplementary Fig. 2A**), and the location of these hyperacetylated regions was largely consistent between different donors (**Fig. 2A**, 'Shared' peaks). Butyrate treatment did not affect overall coverage of H3K4Me2 (**Fig. 2A**, right panel, **Supplementary Fig. 2B**), a histone mark also associated with active chromatin yet not an HDAC target. In addition to coverage per megabase (Mb) of DNA, butyrate treatment increased the number of individually called H3K27Ac peaks in primary human mast cells ~2.6-fold (from 54,710 to 143,799) after 24 h, while H3K4Me2 peaks showed a much more modest increase (~1.3-fold, from 80,219 to 105,037 at 24 h) (**Fig. 2B**). Furthermore, butyrate treatment shifted the relative abundance of acetylation at genomic locations from TSS regions (from ~17% down to ~10%) to intronic and intergenic regions (**Supplementary Fig. 2B**).

In conclusion, these data strengthen the notion that butyrate has a profound effect on genome-wide H3K27Ac histone acetylation dynamics via HDAC inhibition. Notably, these effects occurred without large-scale indirect effects on other histone modifications such as H3K4Me2.

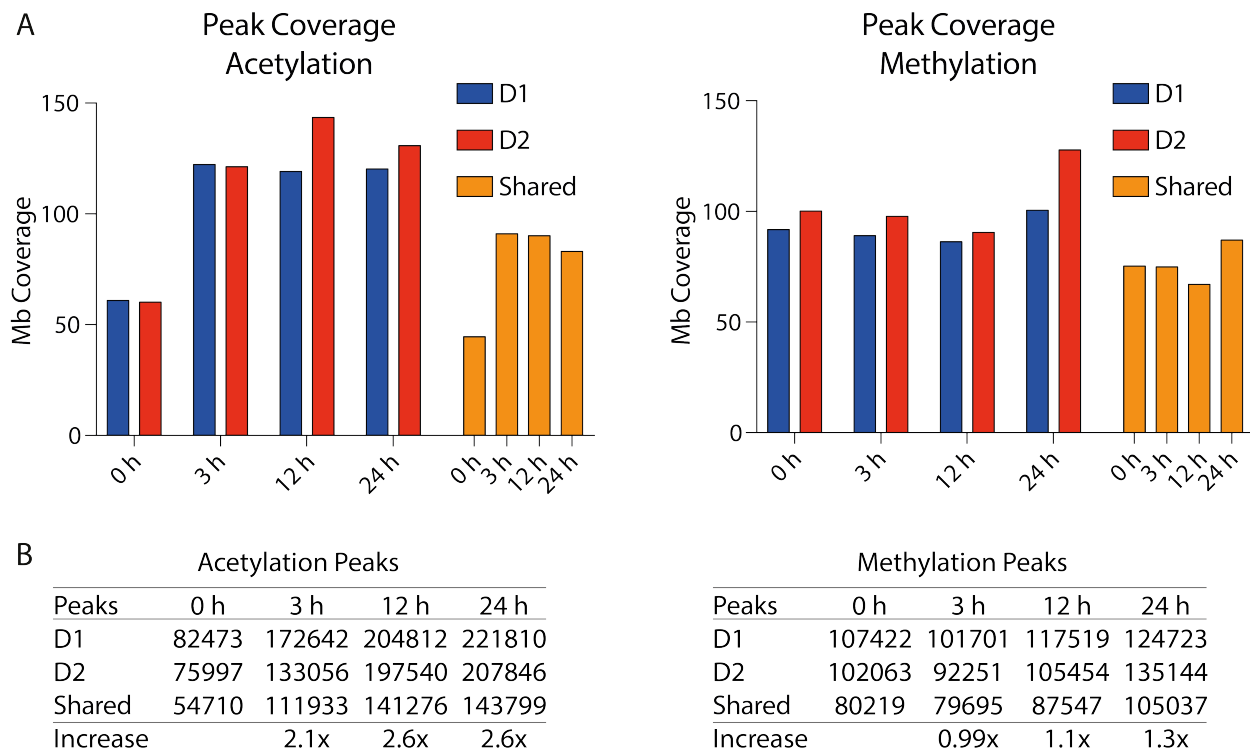


Figure 2. Butyrate triggers global histone hyper-acetylation without large-scale indirect effects on other histone modifications. Chromatin immunoprecipitation (ChIP)-Seq for histone 3 lysine 27 acetylation (H3K27Ac) and histone 3 lysine 4 di-methylation (H3K4Me2) was performed after 0, 3, 12 and 24 hours of butyrate treatment. **(A)** Megabase (Mb) coverage of histone acetylation (H3K27Ac, left) and methylation (H3K4Me2, right). Donor 1 (D1) is indicated in blue and donor 2 (D2) is indicated in red. Overlap between the donors is indicated by the shared peaks (yellow bars). **(B)** Total number of called acetylation (left) and methylation (right) peaks following butyrate treatment in donor 1 and donor 2, with shared peaks and increases in peak count (based on shared peak counts) indicated.

Distinct patterns of histone acetylation dynamics induced by butyrate

To gain a more quantitative picture of H3K27Ac dynamics upon butyrate treatment, we performed differential enrichment analyses with DESeq2 on reproducible peaks, which showed that most regions acetylated at baseline (>68%) were not significantly (fold change > 2 and adjusted P value < 0.05) affected by 3-24 h butyrate treatment (**Supplementary Fig. 3**). After 3 h exposure, butyrate mostly triggered hyper-acetylation (6.3% hyper-acetylated vs. 2.2% hypo-acetylated peaks), whereas 12 h butyrate exposure showed similar proportions of hyper- and hypo-acetylation at baseline H3K27Ac+ regions (13.3% vs. 12.8%). Finally, 24 h of treatment mostly induced hypo-acetylation of existing peaks (13.1% vs. 18.6%, **Supplementary Fig. 3**).

To better annotate at which regulatory sites butyrate-induced histone acetylation dynamics occur, we intersected regions of dynamic acetylation with TSS locations and putative typical enhancer or super-enhancer regions as defined by the ROSE algorithm^{28,35}. At untreated conditions (indicated as 0 h), histone acetylation was primarily located distant from TSS regions, with the bulk of H3K27Ac+ sites located 50-500 kb away from the TSS (**Fig. 3A**, bar graph). Furthermore, ~52% and ~19% of acetylated peaks were associated with typical enhancers and super-enhancers, respectively, whereas 17% of acetylated peaks were associated with TSS regions (**Fig. 3A**, donut graph).

A 3 h exposure to butyrate led to 1226 significantly hypo-acetylated peaks, which were predominantly located near TSSs (**Fig. 3B**, within +/- 5kb). In fact, ~48% of all hypo-acetylated regions were located at a TSS (**Fig. 3B**, left donut graph). Although the total number of hypo-acetylated peaks strongly increased with prolonged butyrate exposure (8.8-fold increase), their location remained disproportionally enriched at TSS regions (**Fig. 3B-D**). Oppositely, butyrate treatment for 3 h led to 3547 significantly hyper-acetylated peaks, which were predominantly located distal of TSS regions (**Fig. 3B**, >5kb upstream or downstream). Overall, ~55% of all hyper-acetylated regions intersecting with a typical enhancer, and ~21% intersecting with a super-enhancer (**Fig. 3B**, right donut graph). Although the number of hyper-acetylated peaks increased with prolonged butyrate exposure (2.1-fold increase), their location remained disproportionally enriched at enhancer locations (**Fig. 3B-D**). Specifically, 12 and 24 h after butyrate treatment, ~86% of all hyper-acetylated peaks were located either at a typical enhancer or super-enhancer (**Fig. 3C, D**).

These data reveal that butyrate – despite its potent capacity for HDAC inhibition – affects histone acetylation at a relatively small subset (i.e. ~30%) of pre-existing H3K27Ac+ chromatin regions. Strikingly, butyrate-induced HDAC inhibition preferentially reduces H3K27Ac levels at TSSs, while H3K27Ac enrichment primarily occurs at locations distal from TSS regions, co-localizing with typical enhancers and super-enhancers.

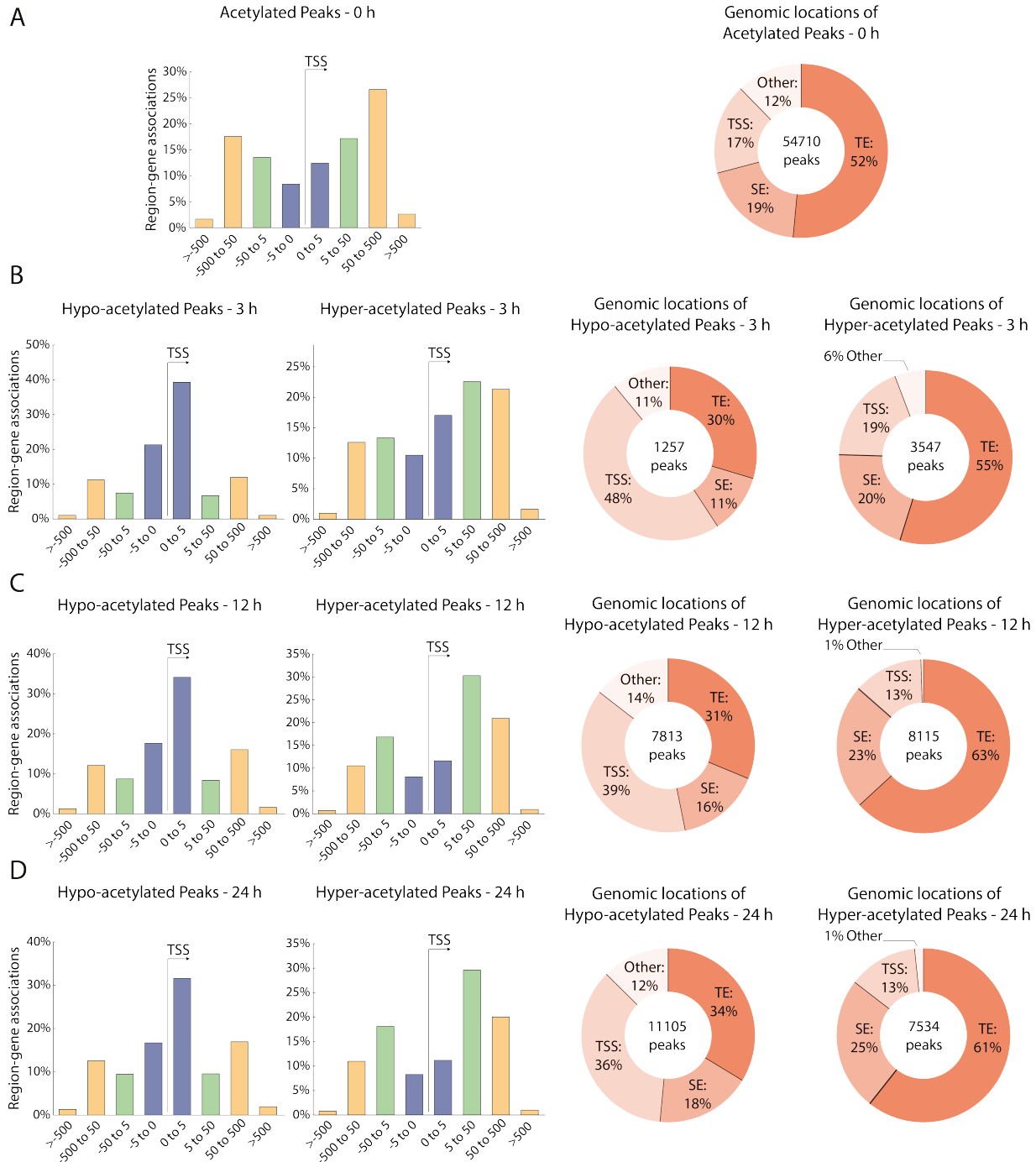


Figure 3. Butyrate induces distinct patterns of histone acetylation dynamics. (A) Distance of acetylated peaks in untreated human mast cells (0h) to associated transcription start site (TSS) regions, both upstream (left side) and downstream (right side). Distances of peak to TSS from 0 to 5 kb are indicated in purple, 5 – 50 kb in green and distances greater than 50 kb are indicated in yellow. Donut plots indicate the genomic locations of differentially acetylated regions, which were defined as typical enhancers (TE), super-enhancers (SE, identified using ROSE), TSS regions (TSS) or other. (B-D) Same analysis as in A but for mast cells treated with butyrate for 3 (B), 12 (C) and 24 (D) hours. Differential enrichment was calculated using DESeq2 on reproducible peaks (fold change > 2 and adjusted P value < 0.05).

Differential impact of butyrate on acetylation dynamics at transcriptionally activated or repressed loci

We next assessed how the observed changes in histone acetylation upon butyrate treatment translate into altered gene expression. We observed hypo-acetylated TSS peaks near several downregulated genes, including the mast cell activation-associated genes BTK (3.97 fold decrease expression), SYK (3.89 fold), MRGPRX2 (4.86 fold) and KIT (2.45 fold) (**Fig. 4A**). Overall acetylation at the TSS of the 864 (**Fig. 1B**) downregulated genes was strongly and immediately reduced upon butyrate exposure (**Fig. 4B**, left histogram). Although TSS acetylation was also reduced at transcriptionally unchanged genes (defined as the 600 genes with the lowest fold change in expression after butyrate treatment) and the 551 upregulated genes (**Fig. 4B**, middle and right histogram), the quantitative reduction in area under the curve was strongest and fastest for the 864 downregulated genes (**Fig. 4C**).

We also tested whether increased histone acetylation upon butyrate treatment was linked to elevated gene expression levels. Several strongly upregulated genes (Log2 fold change > 4) displayed hyper-acetylation at their TSS regions (representative examples are F2RL1 and CLGN, which show 1500 and 675 fold increased expression respectively; **Fig. 4D**). Indeed, acetylation at the TSS of the 50 most upregulated genes was increased at all measured timepoints (**Fig. 4E**, left histogram). Acetylation at the TSS of a broader set of the 100 most upregulated genes was also increased at 3 h after butyrate exposure, although H3K27Ac levels returned to near basal levels after 12 and 24 h (**Fig. 4E**, middle histogram). However, the 451 remaining upregulated genes, which showed weaker induction and higher baseline TSS acetylation, showed reduced TSS H3K27Ac signals in response to prolonged (>3 h) butyrate treatment (**Fig. 4E**, right histogram). Area under the curve quantification validated that acetylation at the TSS of strongly upregulated genes rapidly increased, whereas acetylation at the TSS of moderately or weakly upregulated genes actually decreased (**Fig. 4F**). Notably, the most strongly upregulated genes (i.e. top 50/100) displayed lower baseline acetylation (**Fig. 4E**) and RNA expression (**Supplementary Fig. 4**), whereas less strongly upregulated genes had established TSS acetylation and higher expression prior to butyrate treatment (**Supplementary Fig. 4**). These results suggests that transient hyper-acetylation at the TSS of genes may be sufficient to induce gene activation at poorly expressed or silent genes, whereas the butyrate-mediated induction of already robustly expressed genes is regulated by TSS acetylation-independent mechanisms.

As the majority of hyper-acetylated peaks were located at typical enhancers (**Fig. 3B-D**), we next quantified changes in acetylation enrichment in the enhancer landscape (EL, defined as all non-TSS H3K27Ac peaks). Histone acetylation at the EL linked to the 864 downregulated and unchanged genes displayed an initial modest increase, but decreased again after 24 h (**Fig. 4G**, left and middle histogram). Acetylation at the EL around the 551 upregulated genes was increased at all measured timepoints (**Fig. 4G**,

right histogram), which was supported by quantification of the area under the curve (**Fig. 4H**).

Taken together, these findings demonstrate that butyrate exposure induces complex histone acetylation dynamics. Generally, H3K27Ac was rapidly depleted around the TSS of genes, which was most pronounced for downregulated genes. Only very strongly induced genes expressed at very low baseline levels did show a sustained gain in promoter H3K27Ac levels. The overall effects on the enhancer landscape appear to be more modest, although hyper-acetylation of enhancers may, in part, be linked to the upregulated expression of associated genes.

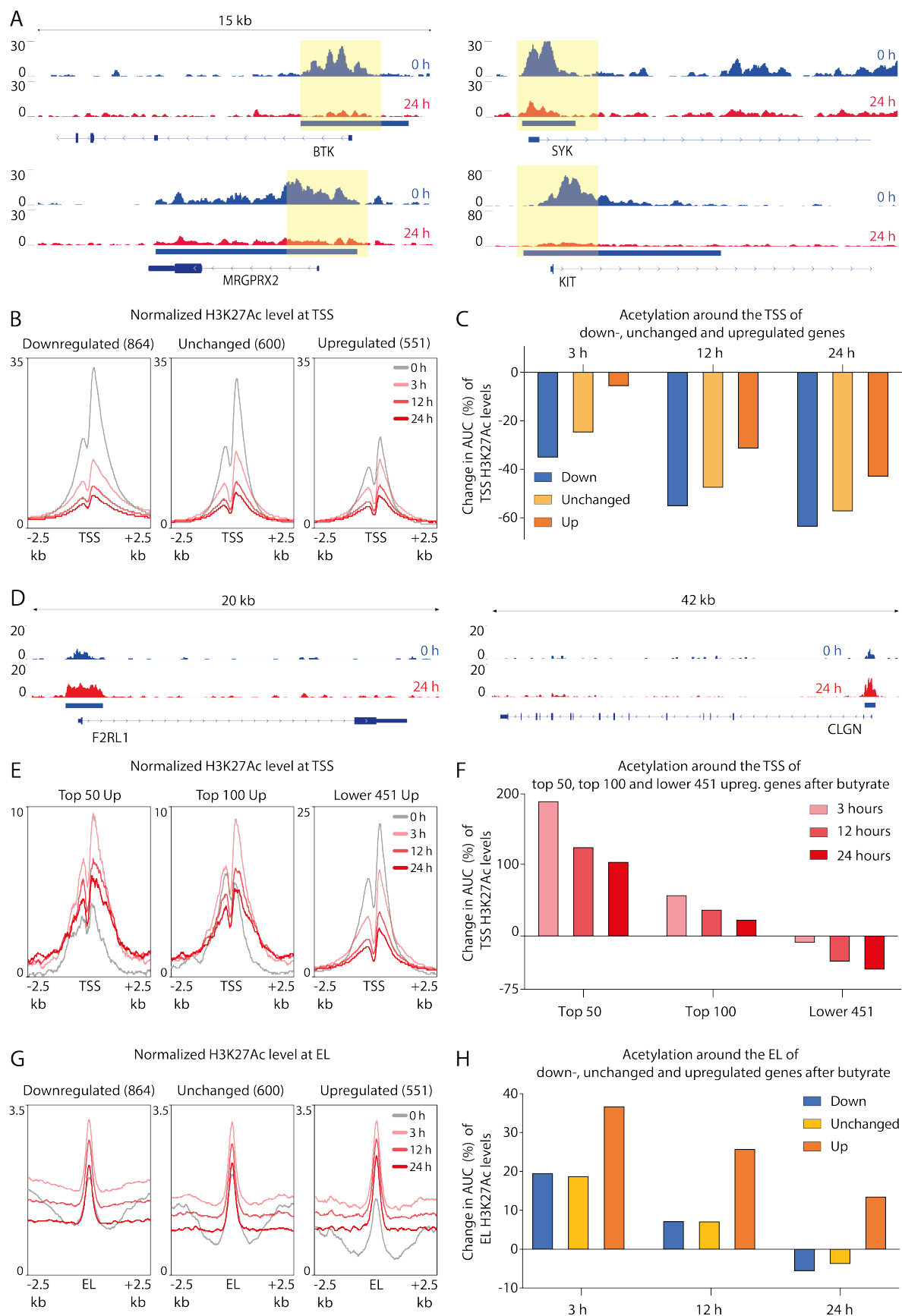


Figure 4. Butyrate exposure induces complex histone acetylation dynamics that only partially correlate with transcriptional outcomes. RNA-Seq and ChIP-Seq datasets, obtained from butyrate-treated primary human mast cells, were integrated to investigate the relationship between butyrate-mediated controls of histone acetylation and gene expression. **(A)** Representative examples of hypo-acetylated (indicated by a blue rectangle) canonical mast cell genes (i.e. *BTK*, *SYK*, *MRGPRX2* and *KIT*). Yellow shading highlight significant differences between histone acetylation in untreated human mast cells (indicated in blue, 0 h) and butyrate treated human mast cells (indicated in red, 24 h). **(B)** Histograms of H3K27Ac at the TSS of downregulated genes (left box), unchanged genes (middle box) and upregulated genes (right box). The 0 h timepoint is indicated in light grey and TSS acetylation after butyrate treatment indicated in shades of red. **(C)** Quantification of the reduction of TSS acetylation area under the curve at 3, 12 and 24 h after butyrate treatment (with downregulated genes indicated in blue, unchanged genes in yellow and upregulated genes in orange). **(D)** Examples of hyper-acetylated genes (i.e. *F2RL1* and *CLGN*). **(E)** Histograms of H3K27Ac at the TSS of the top 50 upregulated genes (left box), top 100 upregulated genes (middle box) and lower 451 upregulated genes (right box). **(F)** Area under the curve quantification of data shown in E. **(G)** Histograms of H3K27Ac at the enhancer landscape (EL) of downregulated genes (left box), unchanged genes (middle box) and upregulated genes (right box). **(H)** Area under the curve quantification of data shown in G.

Butyrate preferentially suppresses super-enhancers and their associated genes

Because super-enhancers can be extensively acetylated and have been reported as preferential targets of HDAC inhibitors^{36,37}, we next investigated H3K27Ac dynamics at super-enhancers and transcriptional changes of their target genes. From two biological replicates, 608 reproducible super-enhancers were identified that were linked to 588 unique associated genes in untreated primary human mast cells (**Fig. 5A**). These genes were strongly enriched for immune effector cell processes, such as cell activation, exocytosis and secretion (**Fig. 5B**). These included super-enhancers associated with *CD9*, *LAIR1*, *COTL1* and *LAT*, which are known regulators of mast cell mediator secretion (**Fig. 5C**), as well as other mast cell-associated genes such as *KIT*, *MS4A2* and *LYN* (**Supplementary Table 2**).

Most super-enhancers (~84%) overlapped with non-TSS regions that were hypoacetylated (fold change > 2 and adjusted P value < 0.05) after 24 hours of butyrate treatment (**Fig. 5C,D**). Pathway enrichment analyses of the 502 genes associated with hypo-acetylated super-enhancer revealed that they are particularly associated with regulation of cell activation, FCER1 mediated Ca²⁺ mobilization and mast cell mediated immunity (**Fig. 5E**). Of note, ~19% of hypo-acetylated super-enhancers were linked to transcriptionally downregulated genes (**Fig. 5F**), as compared to only 6-8% for hypo-acetylated typical enhancers and TSS regions. For genes expressed prior to butyrate treatment (RPKM>1), hypo-acetylation of super-enhancers represented the strongest predictor of transcriptional downregulation (24%), followed by hypo-acetylation of typical enhancers (13.0%) and TSS regions (7.7%) (**Supplementary Fig. 5A**).

Genes that displayed downregulated expression and super-enhancer hypo-acetylation (n=95, 18.9% of 502 genes) were strongly associated with (mast cell) activation and exocytosis (**Fig. 5G**). By contrast, downregulated genes linked to hypo-acetylated typical enhancer regions associated with more general immune functions (**Supplementary Fig. 5B**). Together, these findings provide a plausible epigenetic explanation for the transcriptional deregulation of many downregulated genes, i.e., via loss of histone acetylation of their TSSs, super-enhancers, or both (**Fig. 5H**). Of note, out of the 864 downregulated genes, 112 genes were associated with super-enhancers, a majority (85%) of which displayed hypo-acetylation after 24 hours of butyrate.

A considerable share of hyper-acetylated peaks was located in super-enhancer regions (~21-25%) (**Fig. 3B-D**), and ~20% of super-enhancers contained a hyper-acetylated region after 24 hours of butyrate treatment (**Supplementary Fig. 5C**). Yet, only ~0.4% of hyper-acetylated super-enhancers were linked to transcriptionally upregulated genes, similar to hyper-acetylated typical enhancers and TSS regions (**Supplementary Fig. 5D**). Instead, weak hyper-acetylation (i.e. not passing our thresholds for differential enrichment) at typical enhancers may better explain why expression is induced at such genes (**Supplementary Fig. 5E, F**).

In summary, these data indicate that super-enhancers are an important target of butyrate-induced HDAC inhibition, most often resulting in a loss of H3K27Ac and correlating with reduced expression of many associated key mast cell genes.



Figure 5. Butyrate perturbs super-enhancers and preferentially suppresses SE-associated transcripts. (A) Super-enhancers (SE) were ranged by H3K27Ac signal in untreated human mast cells of donor 1 (left hockey stick graph) and donor 2 (right hockey stick graph). (B) Pathway enrichment analysis of 588 consistent (present in both donor 1 and 2) SE genes in untreated human mast cells. (C) Representative examples of SE (indicated by yellow rectangles) in untreated human mast cells (0 h, indicated in blue), that become hypo-acetylated (indicated by green bars) in response to butyrate treatment (24 h, indicated in red). Overlap between identified SE and hypo-acetylated regions is indicated by red bars (intersect). (D) Proportion of SE that contain hypo-acetylated regions (in blue) and SE regions that do not intersect with a hypo-acetylated region (in light red). (E) Pathway enrichment analysis of 502 hypo-acetylated SE genes. (F) The percentage of hypo-acetylated SE, typical enhancer (TE) or TSS regions linked to a downregulated gene. (G) Pathway enrichment analysis of 95 downregulated genes associated with hypo-acetylated SE regions. (H) Epigenetic explanation for butyrate-induced downregulation of gene expression. The proportion of downregulated genes with significant hypo-acetylated TSS (purple), TSS and SE (green), SE (yellow) and non-significant reduced acetylation (pink). Differential enrichment was calculated using DESeq2 (fold change > 2 and adjusted P value < 0.05).

Human mast cell activation is regulated by super-enhancer activity and the associated cell-type specific transcriptional networks.

Next, we set out to assess whether specific perturbation of super-enhancer activity can indeed affect human mast cell activation. To this end we treated primary human mast cells with JQ-1, a bromodomain containing 4 (BRD4) inhibitor³⁸, and induced degranulation by IgE/antigen stimulation. BRD4 is highly enriched at super-enhancer regions and actively regulates the expression of associated genes³⁹. JQ-1 potently inhibited primary human mast cell degranulation, in a concentration-dependent manner (**Fig. 6A**). JQ-1 did not induce cell death at the tested concentrations (data not shown). To assess whether the effects of JQ-1 were (non-)additive to the effects of butyrate on human mast cell activation, suboptimal concentrations of JQ-1 (50ng/mL) and butyrate (1mM), as well as a combination of the two inhibitors, were incubated with the cells for 24 h followed by IgE crosslinking. Inhibition of mast cell degranulation by butyrate was not further increased by (low-dose) JQ-1 addition, suggesting that both inhibitors target the same modulators of human mast cell activation (**Fig. 6B**). Indeed, JQ-1 repressed expression of various super-enhancer associated genes that were also repressed by butyrate (**Fig. 6C, Supplementary Fig. 6A**). LAIR, LCP2, LAT and LAT2 are essential modulators of human mast cell activation^{40–43}, which may explain why mast cells display an inhibited degranulation profile after both butyrate and JQ-1 exposure.

A simple explanation for preferential deacetylation at TSS and super-enhancer regions after butyrate treatment may be a non-selective redistribution of histone acetylation that affects such regions more profoundly due to their extensively acetylated nature. However, a substantial number of established highly enriched H3K27Ac peaks either increased in acetylation levels or – even more frequently – were unaffected by butyrate treatment (representative examples in **Supplementary Fig. 6B**). For example, only ~31% of the 500 most extensively acetylated sites in the mast cell genome were hypo-acetylated by butyrate after 3 h (**Supplementary Fig. 6C**). Nevertheless, most hypo-acetylated peaks (~74%; 890 out of 1203) after 3 h treatment originated from the 5000 strongest H3K27Ac peaks (**Supplementary Fig. 6D**). Thus, butyrate-induced hypo-acetylation selectively targets a subset of extensively acetylated peaks.

Taken together, these data indicate that human mast cell activation is strongly regulated by super-enhancer activity and the associated cell-type specific transcriptional networks. Furthermore, butyrate likely exerts (part of) its inhibitory effects on human mast cell activation via the specific perturbation of super-enhancer activity.

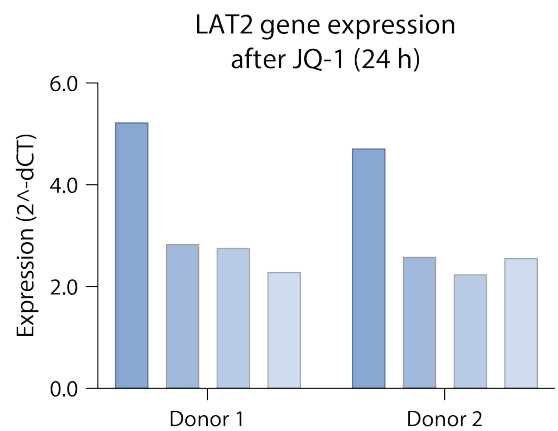
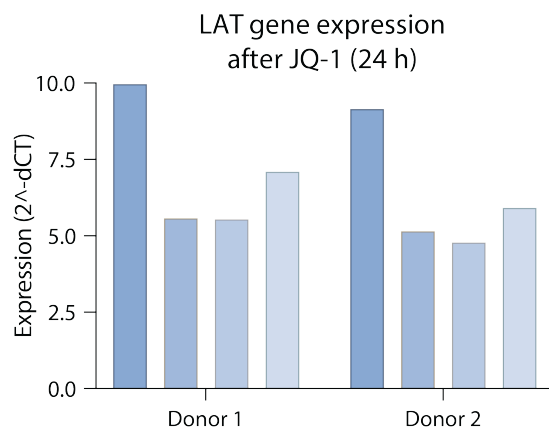
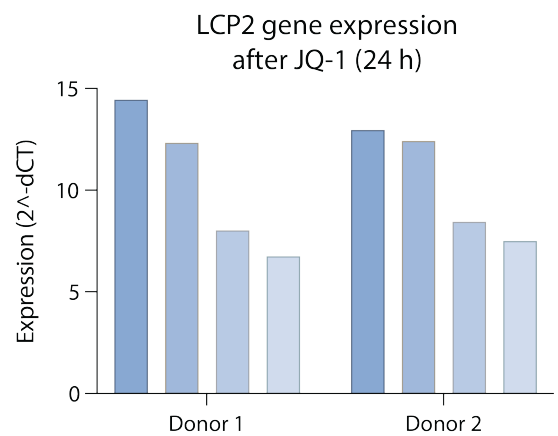
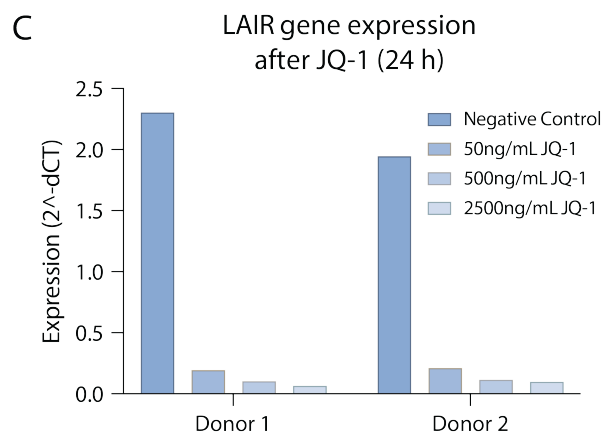
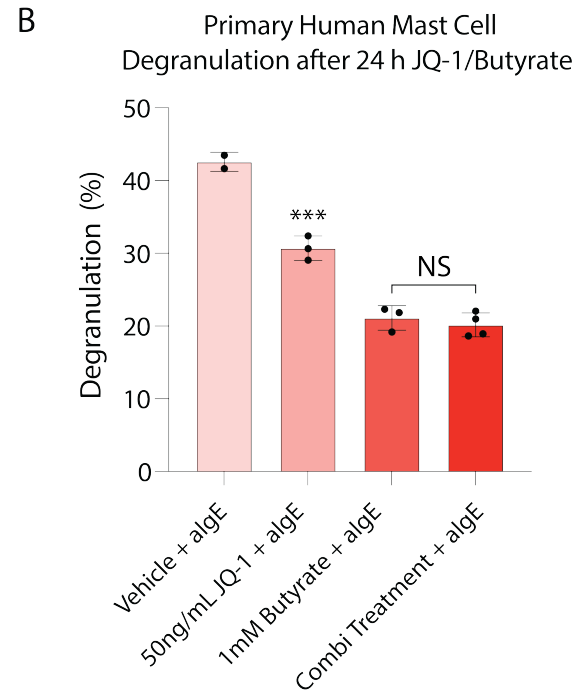
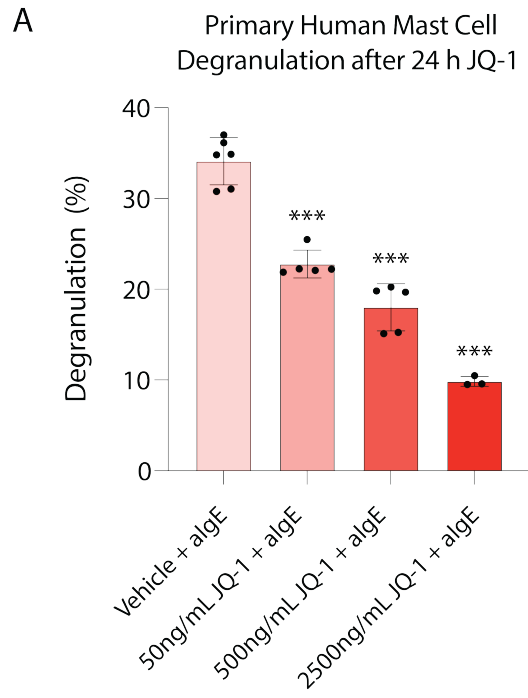


Figure 6. BET-bromodomain inhibitor JQ-1 inhibits human mast cell activation to a similar extent as butyrate. (A) Primary human mast cells were treated with increasing concentrations of JQ-1 for 24 h, primed with IgE and cross-linked with anti-IgE. Percentage of mast cell degranulation (as measured by beta-hexosaminidase release) after IgE-mediated activation using anti-IgE stimulation in primary human mast cells treated with increasing concentrations of JQ-1. (B) Percentage of degranulation after IgE-mediated human mast cell activation in untreated, JQ-1 treated (50ng/mL, 24 h), butyrate treated (1mM, 24 h) or combination treated (JQ-1+butyrate, 24 h) cells. (C) Gene expression ($2^{\Delta\text{CT}}$) of *LAIR*, *LCP2*, *LAT* and *LAT2* in human mast cells derived from two different donors treated with increasing concentration of JQ-1 for 24 h. Data represent mean \pm SD (panel A), statistical significance was tested using a one-way ANOVA test: *Significantly decreased compared with control ($P < .05$). *** $P < .001$. NS, not significant.

Discussion

Although we and others have demonstrated that butyrate and other HDAC inhibitors can regulate the activity of mast cells and other immune cells, it remains incompletely understood how such broadly-acting molecules can exert rather precise and cell-type specific transcriptional changes. By integrating RNA-Seq and ChIP-Seq datasets obtained from butyrate-treated primary human mast cells, we uncovered that butyrate controls mast cell function through complex yet highly specific changes in histone acetylation – including a loss of acetylation at super-enhancers that control key mast cell degranulation genes. Pharmacological inhibition of super-enhancers indeed suppressed mast cell degranulation, similar to what was observed for butyrate.

We found that gene repression following butyrate treatment is primarily associated with H3K27Ac depletion around the TSS of highly expressed genes. Although seemingly counterintuitive, many studies have reported gene repression triggered by HDAC inhibitors⁴⁴. Highly expressed genes were previously shown to be prime targets of HDAC inhibitors in (cancer) cell lines^{45,46}, including KIT in transformed human mast cells⁴⁷, in line with our own findings. This may be explained by preferential binding of HDACs to highly expressed genes, where they are considered to be critical for maintaining the precise acetylation-deacetylation balance required for productive gene transcription^{46,48}. As histone acetylation attracts many proteins involved in transcriptional control, a global redistribution of histone acetylation, as caused by butyrate, is likely to redirect these chromatin readers away from their target regulatory regions⁴⁶. While our findings agree with these notions, we also show that many highly-expressed and strongly acetylated genes are completely impervious to HDAC inhibition by butyrate, indicating that additional mechanisms determine the remarkable selectivity by which butyrate affects the epigenome and transcriptome of mast cells.

In agreement with findings by Rada-Iglesias et al.⁴⁹, our analysis of H3K27Ac dynamics in mast cells revealed that butyrate-induced hyper-acetylation is mostly an early and transient event, since hypo-acetylation became the dominant effect at 24 hours. This suggests that histone deacetylation might be a secondary effect of HDAC inhibition, as HATs gain a competitive advantage for acetyl groups and are able to deposit these at new locations. In primary human mast cells, loss of H3K27Ac at gene regulatory regions upon butyrate treatment was not caused by notable reductions in HAT expression (data not shown). Important to note here is that a previous study of the HDAC inhibitor largazole revealed that exposure to low concentrations solely induced gene activation, whereas higher concentrations shifted the balance towards gene repression⁵⁰. Whether a similar dose-dependent response exists for butyrate will need to be addressed in subsequent studies.

To our best knowledge, we are the first to define super-enhancers in primary human mast cells, and describe their potential relevance for mast cell biology. Super-enhancer-associated genes in human mast cells were strongly linked to immune effector

cell processes, such as cell activation, exocytosis and secretion. Likely due to their high HDAC and HAT occupancy, ~84% of super-enhancers contained hypo-acetylated regions after butyrate treatment, which correlated with reduced transcriptional output of many nearby genes. Among these affected super-enhancer-associated genes are many core regulators of mast cell identity and function, including the KIT receptor, FcεRI signaling components and degranulation-associated factors. Interestingly, perturbation of super-enhancer activity by JQ-1 inhibited degranulation of primary human mast cells, most likely via downregulation of various key mast cell identity genes that are also targeted for repression by butyrate. Indeed, specific repression of core cell identity gene expression by HDAC inhibitors has been previously reported^{50,51}. Thus, it appears plausible that at least part of the inhibitory effect of butyrate is a direct consequence of super-enhancer destabilization. How mast cell activation subsequently reorganizes the chromatin landscape, a phenomenon recently described by Cildir et al⁵², and which specific (combination of) repressed genes form the foundation of butyrate's inhibitory effects, are important topics for future studies.

In summary, our data indicate that butyrate inhibits mast cell activation via a surprisingly selective suppression of the core mast cell transcriptional program, in part by targeting super-enhancers. Acquiring a deeper understanding of the mechanisms of action of butyrate, and other HDAC inhibitors, may in the future offer improved ways to combat mast cell-mediated diseases such as allergies and asthma.

Methods

Peripheral blood mononuclear cell-derived human mast cells

Human peripheral blood mononuclear cell-derived mast cells were generated as previously described by Folkerts et al.³³ Briefly, peripheral blood mononuclear cells were obtained from buffy coats of healthy blood donors and CD34⁺ precursor cells were isolated using the EasySep Human CD34 Positive Selection Kit (STEMCELL Technologies). CD34⁺ cells were maintained for 4 weeks under serum-free conditions using StemSpan medium (STEMCELL Technologies) supplemented with recombinant human IL-6 (50 ng/mL; Peprotech), human IL-3 (10 ng/mL; Peprotech), and human Stem Cell Factor (100 ng/mL Peprotech). Thereafter, the cells were maintained in IMDM Glutamax I containing sodium pyruvate, supplemented with 0.1% 2-mercaptoethanol, 0.5% BSA, 1% insulin- 175 transferrin selenium (all from Invitrogen), ciprofloxacin (10 µg/mL; Sigma-Aldrich), IL-6 (50 ng/mL; Peprotech), and human Stem Cell Factor (100 ng/mL; Peprotech). After 8-12 weeks, PBCMCs were tested for maturity by Giemsa or toluidine blue staining and beta-hexosaminidase release assays.

RNA-Seq gene expression analysis and pathway enrichment analyses

To prepare RNA samples for RNA-seq, total RNA was isolated from human PBCMCs treated with 5 mM butyrate (or vehicle) for 24 h, using the RNeasy Micro Kit (74004, Qiagen). High-throughput sequencing was performed on the Illumina HiSeq 4000 sequencer. Reads were generated of 50 base-pairs in length and alignment was performed using HISAT (Hierarchical Indexing for Spliced Alignment of Transcripts). Tag directories were generated for each sample with removal of duplicate reads (-tbp 1 option). Quantification and normalization of the RNA-Seq data was performed using the open-source software HOMER⁵³. Differential expression was calculated using DESeq2 within the environment of HOMER. Significant differentially expressed genes were defined as differential genes with an adjusted P value < 0.05 (Wald test). To filter out significant differences among lowly expressed genes, an average RPKM value higher than 1 in at least one condition was required. The remaining genes all had a Log2 fold change higher than (-)0.8, we tolerated this cut-off for further downstream analyses. Pathway enrichment analysis was done using Metascape⁵⁴.

ChIP-Seq and data analysis

Chromatin Immuno Precipitation (ChIP) was performed as previously described⁵⁵, with minor modifications. Per ChIP, 100K crosslinked mature primary human mast cells were used. Sonicated chromatin was immunoprecipitated using 1 µg of anti-H3K27Ac antibody (Abcam, Ab4729), 1 µg of anti-H3K4Me2 antibody (Abcam, Ab32356) and 25 µl BSA-blocked Protein A agarose beads (Millipore #16-125). Illumina sequencing libraries were prepared using the ThruPLEX DNA-Seq Kit (Rubicon Genomics) and sequenced on an Illumina HiSeq2500 sequencer (single read 50 bp length, 17-21 million reads per sample).

Reads were aligned to the human GRCh38 genome build using HISAT2⁵⁶ with standard parameters and parsed to HOMER⁵³ for downstream analyses. Tag directories were generated for each sample with removal of duplicate reads (-tbp 1 option). BedGraph files displaying normalized counts (reads per million) were generated for direct visualization in the UCSC Genome Browser using the makeUCSCfile HOMER script. H3K27Ac enriched regions were identified using HOMER findPeaks with -region -size 150 -minDist 370 (parameter set 1) or -region -size 1000 -minDist 2500 (parameter set 2) options. Histograms of ChIP signals were generated with the annotatePeaks script (using the -hist option). ChIP-Seq datasets were deposited in the Gene Expression Omnibus (GEO), accession number pending. Differential peaks were calculated using DESeq2 using default settings (fold change > 2 and adjusted P value < 0.05). Intersect peak files of two different peak files were analyzed via the Genomic Regions Enrichment of Annotations Tool (GREAT), to obtain the distance to associated TSS data. Genomic locations of (differentially) acetylated regions were annotated using the ROSE algorithm and HOMER.

Analysis of super-enhancers and typical enhancers

H3K27ac ChIP-seq data were used for identifying typical and super- enhancers using ROSE software^{28,35}. The H3K27ac ChIP-seq peaks in untreated and treated mast cells were stitched within 12.5 kb of each other and excluding 2.5 kb upstream and downstream of the known transcription start sites (TSS). The combined H3K27ac reads within stitched regions were plotted in a ranked enhancer order. Super-enhancers were defined as the enhancers above the inflection point and the rest were defined as typical enhancers. Annotation of enhancers was performed using the annotatePeaks.pl function (default settings) in HOMER. Pathway enrichment analysis of super-enhancers was performed using Metascape⁵⁴. Differential peaks within super-enhancer regions that overlapped with a TSS region were excluded from downstream analyses.

Mast cell activation assay & Quantitative real-time PCR

Mast cells were cultured (if applicable) with JQ-1 (HY-13030, MedChemExpress) or sodium butyrate (303410, Sigma-Aldrich) 24 h prior to activation. PBCMCs from two different donors were sensitized with human IgE (2 µg/ml, for 1 hour) and washed, followed by stimulation with 2 µg/ml of anti-IgE. Human IgE myeloma was purchased from Milipore-Sigma (401152) and rabbit anti-human IgE from Bethyl Laboratories (A80-109A). Degranulation was measured by the release of beta-hexosaminidase⁵⁷. Substrate 4-MUG (M2133, Sigma-Aldrich) was added to this enzyme containing supernatant and the product was measured after 1 h by means of fluorescence (Glomax Discover, Promega). After RNA isolation as stated above, cDNA was made using RevertAid H Minus First Strand cDNA Synthesis Kit (#K1632, Thermo Fisher Scientific) according to manufacturer. qPCR is performed using PowerUp™ SYBR™ Green Master Mix

(#A25741, Thermo Fisher Scientific) and primers were found by OriGene (Table 1). Run on QuantStudio™ 3 Real-Time PCR System (A28567, Thermo Fisher Scientific).

Table 1 - Quantitative real-time PCR primers

gene name	forward	reverse	Gene ID OriGene
Lair1	TGGTCTGAGCAGAGTGACTACC	GCTCATTGTGACTGTTGTCCGAC	3903
LCP2	GGAAGAAGCCACCTGTGCCAAA	GCTCATAGGAAGTAGTGCTGGC	3937
Lat	ATCCTGGAGCGGCTAAGACTGA	GTTTCAGCTCCTGCAGATTCTCG	27040
Lat2	GCAAGCAGAAAACACAGAGACA	AGAGGGACAGAGACCAGAAGTG	7462
HPRT	ATTGTAATGACCAGTCAACAGGG	GCATTGTTTTGCCAGTGTCAA	home made

Statistical analysis

Statistical tests were performed with Graphpad Prism 9 (GraphPad Software, Inc). One-way ANOVA tests were performed as described in the respective figure legends. A P-value of less than 0.05 was considered statistically significant.

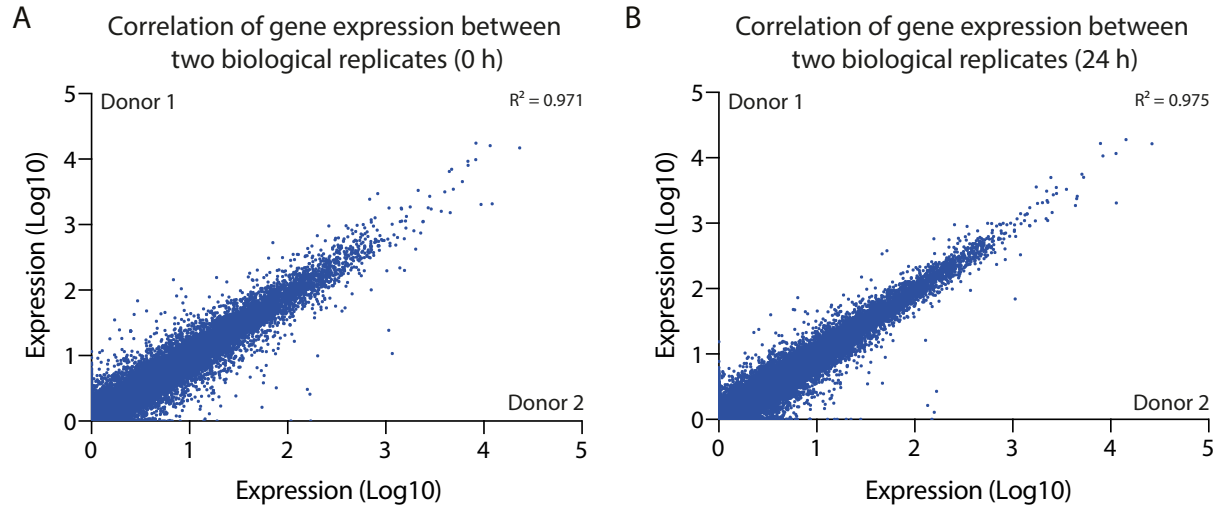
Author Contributions

J.F. performed the experiments with technical assistance of M.B. and W.F.J.v.IJ. J.F. performed data analysis. R.W.H., and R.S. supervised the project and participated in experimental design and technical discussions. J.F. wrote the first draft of the paper. J.F., R.W.H. and R.S. drafted the final manuscript, which was approved by all co-authors.

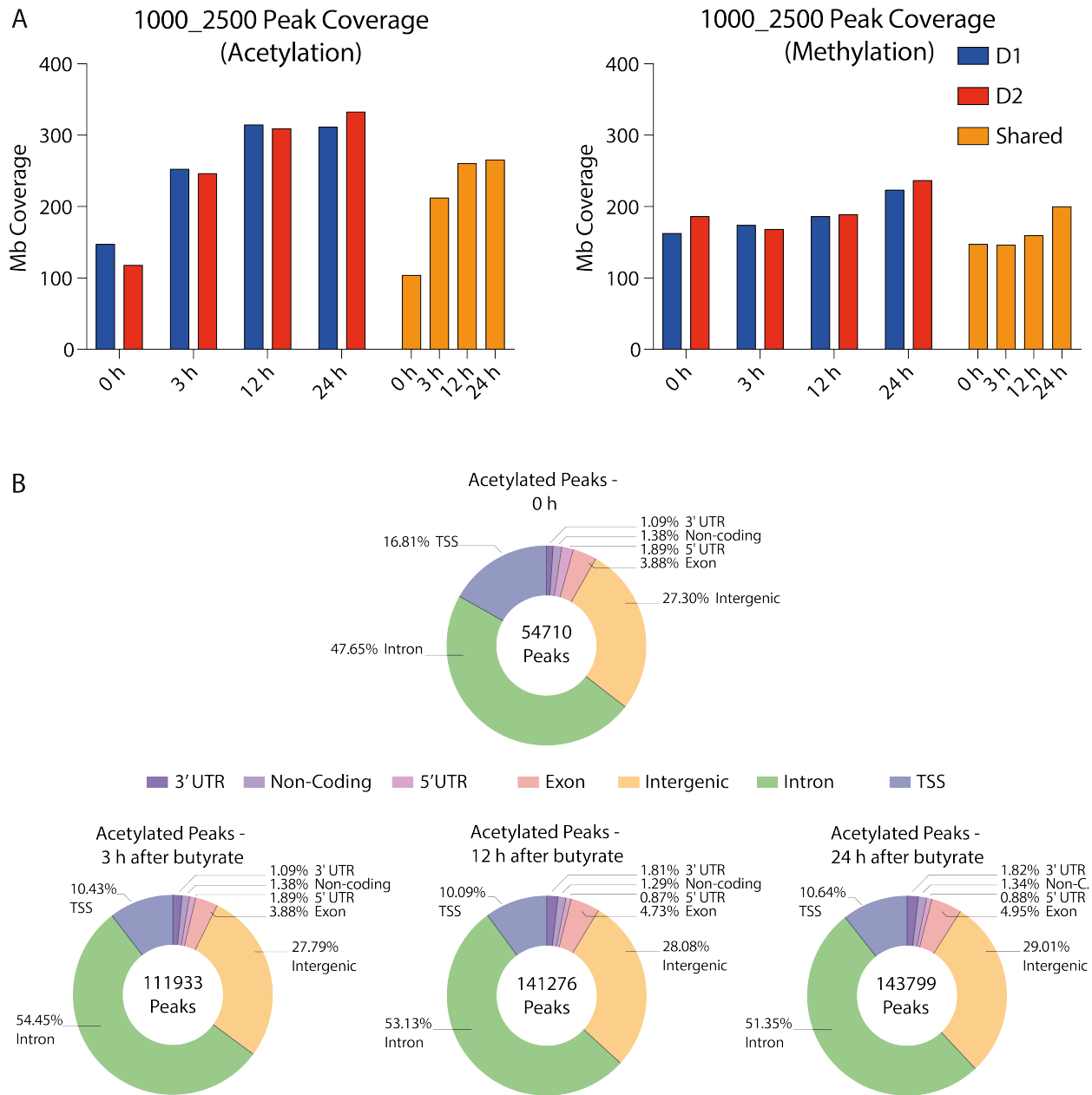
Acknowledgements

We thank Anne van Schoonhoven (Department of Pulmonary Medicine, Erasmus MC) for her advice and technical support during the ChIP-Seq data analysis. J.F. is supported by a EAACI Long-Term Research Fellowship. R.S. is supported by a Dutch Research Council Vidi grant (09150172010068), an Erasmus MC Fellowship, and a Dutch Lung Foundation Junior Investigator grant (4.2.19.041JO). This work was partly supported by the Lung Foundation Netherlands Grant 4.1.18.226 to R.W.H.

Supplementary Information

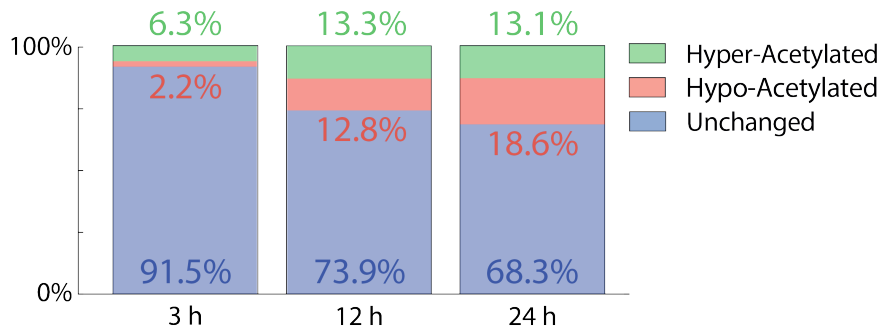


Supplementary Figure 1. Correlation of gene expression values between both primary human mast cell cultures. (A, B), Comparison of gene expression (Log10) profiles between donor 1 and donor 2, in untreated (left scatter plot) and butyrate treated human mast cells (right scatter plot).



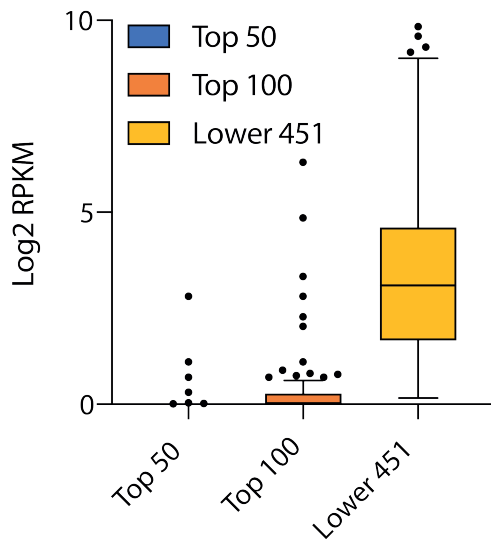
Supplementary Figure 2. Butyrate treatment shifts the relative abundance of acetylation at genomic locations from TSS regions to intronic regions, without affecting histone methylation. Chromatin immunoprecipitation (ChIP)-Seq specific for histone 3 lysine 27 acetylation (H3K27Ac) and histone 3 lysine 4 di-methylation (H3K4Me2) was performed after 0, 3, 12 and 24 h of butyrate treatment. **(A)** Megabase (Mb) coverage of histone acetylation (H3K27Ac, left) and methylation (H3K4Me2, right), using peak-calling parameter settings -size 1000 -minDist 2500. Donor 1 (D1) is indicated in blue and donor 2 (D2) is indicated in red. Overlap between the donors is indicated by the shared bars (yellow). **(B)** Genomic annotation of H3K27Ac peaks in untreated human mast cells (upper donut graph) and redistribution of acetylation peaks induced by 3, 12 and 24 hours of butyrate treatment (lower donut graphs).

Proportion Hyper-, Hypo-, Unchanged Acetylated Peaks

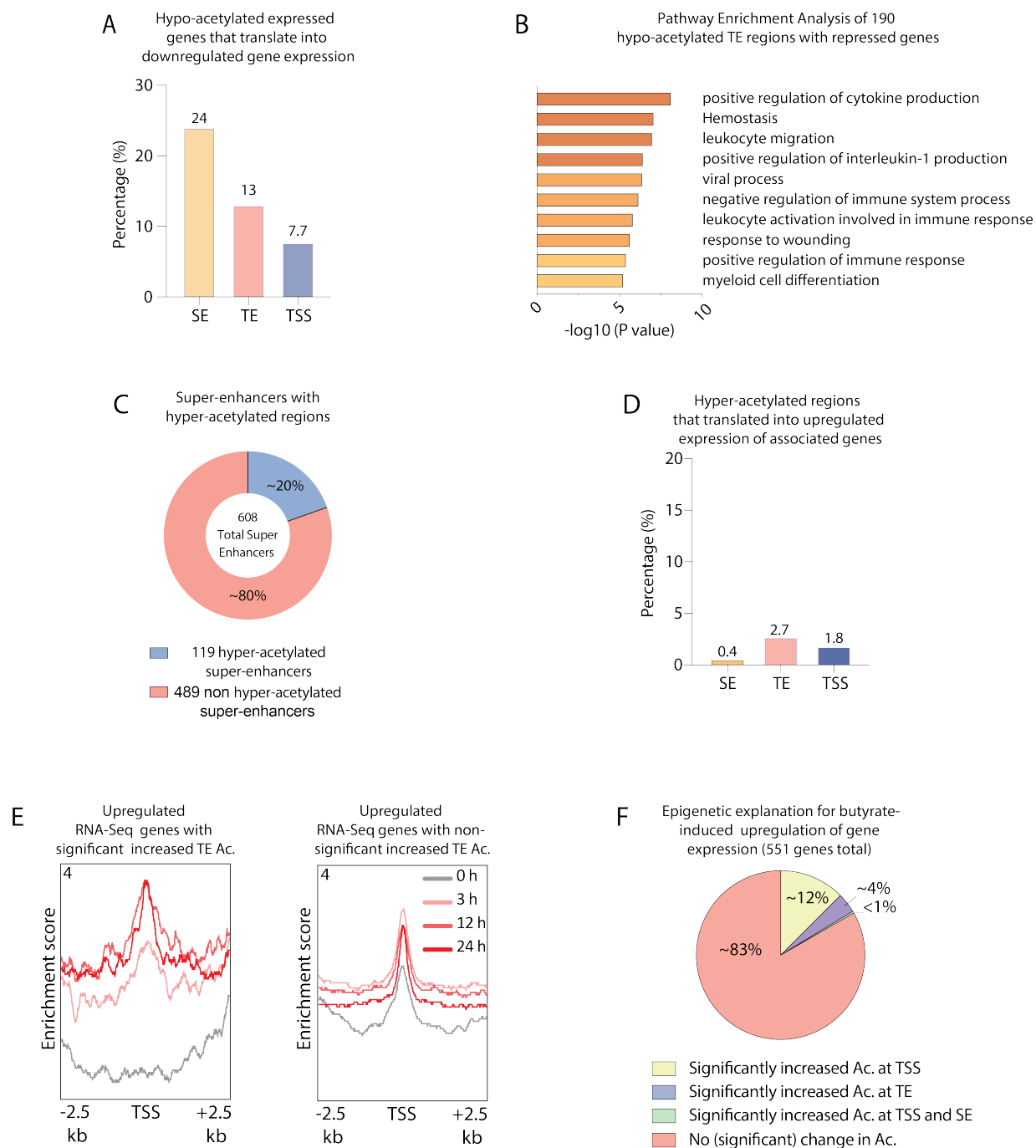


Supplementary Figure 3. Most H3K27Ac+ regions at baseline are not significantly affected by butyrate treatment. Differential enrichment analysis (fold change > 2 and adjusted P value < 0.05) was performed using DESeq2 to gain a quantitative picture of H3K27Ac dynamics upon butyrate treatment. Distribution of hyper-acetylated (in green), hypo-acetylated (in red) and unchanged (in purple) baseline (0 h) H3K27Ac+ peaks in response to 3, 12 and 24 hours of butyrate treatment.

Basal expression of upregulated genes



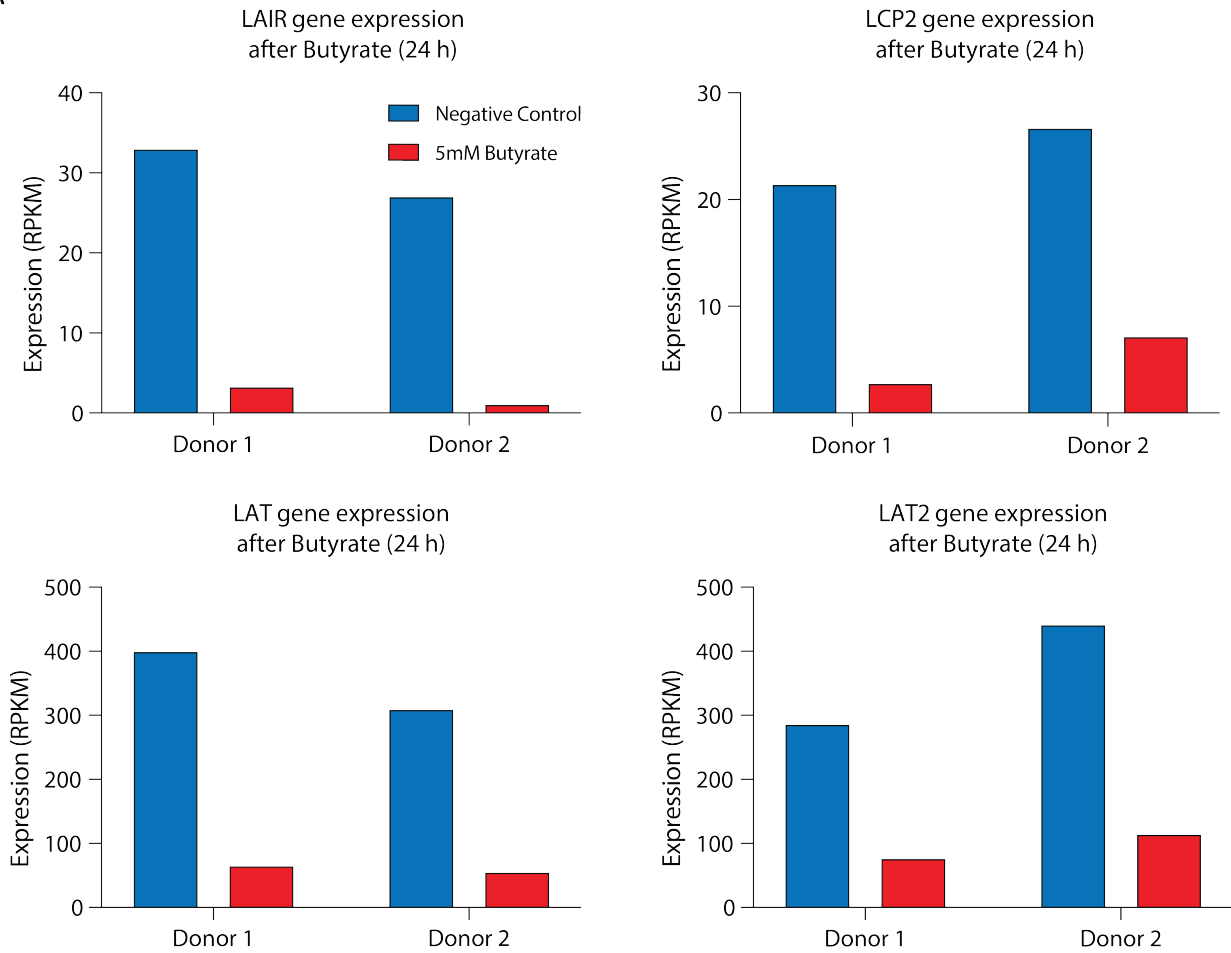
Supplementary Figure 4. Strongly upregulated genes upon butyrate treatment display low levels of baseline acetylation. Comparison of basal expression levels of upregulated genes, distinguishing between the top 50 (in blue), top 100 (in orange) and lower 451 (in yellow) upregulated genes.



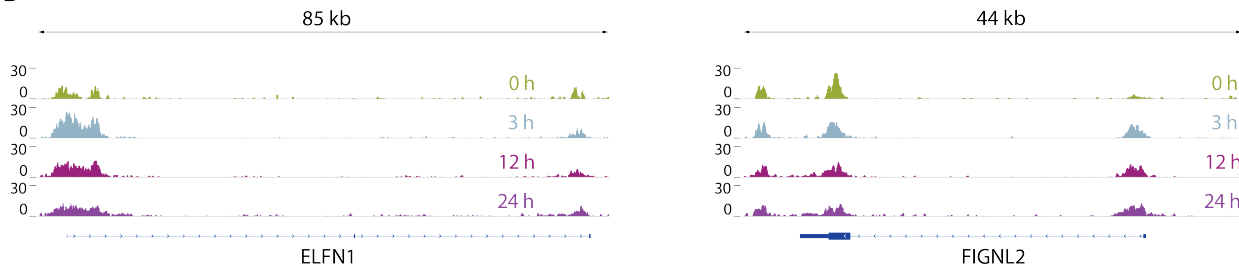
Supplementary Figure 5. H3K27Ac acetylation at super-enhancers and associated transcriptional dynamics. (A) The percentage of expressed hypo-acetylated genes that are downregulated upon butyrate treatment and associated with SE, TE or TSS. (B) Pathway enrichment analysis of 190 hypo-acetylated TE regions with repressed genes. (C) Proportion of identified SE that contain hyper-acetylated regions (in blue) and SE regions that do not intersect with a hyper-acetylated region (in light red). (D) The percentage of hyper-acetylated SE, TE or TSS regions linked to an upregulated gene. (E) Histograms of histone-acetylation at the TSS of upregulated genes with significant (left box) and non-significant (right box) hyper-acetylation at their TEs. The 0 h timepoint is

indicated in light grey and TSS acetylation after butyrate treatment indicated in red. **(F)** Epigenetic explanation for butyrate-induced upregulation of gene expression. The proportion of upregulated genes with significant hyper-acetylated TSS (purple), TSS and SE (green), SE (orange), TE (yellow) and non-significant reduced acetylation (pink).

A



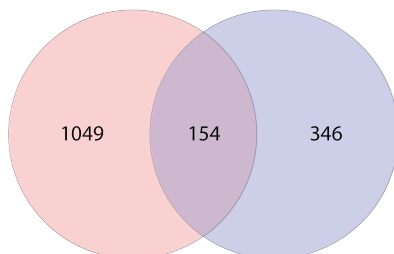
B



C

1203 Hypo-Acetylated Peaks 3 h after butyrate treatment

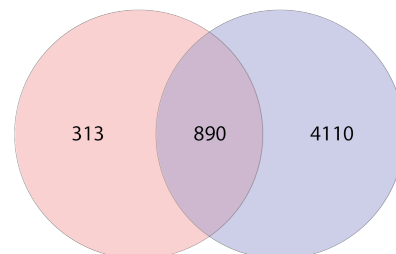
Top 500 Most Acetylated Peaks in resting human mast cells



D

1203 Hypo-Acetylated Peaks 3 h after butyrate treatment

Top 5000 Most Acetylated Peaks in resting human mast cells



Supplementary Figure 6. Extensively acetylated peaks are preferable targets of butyrate-induced hypo-acetylation, but in a selective manner. (A) Gene expression (RPKM) of *LAIR*, *LCP2*, *LAT* and *LAT2* in human mast cells derived from two different donors treated with 5mM Butyrate for 24 h. (B) Genomic browser view of representative examples of unaffected or (transient) hyper-acetylation at established acetylation peaks. (C) Venn diagram comparing the 1203 hypo-acetylated peaks after 3 hours of butyrate treatment with the top 500 most acetylated peaks in the mast cell epigenome. (D) Venn diagram comparing the 1203 hypo-acetylated peaks after 3 hours of butyrate treatment with the top 5000 most acetylated peaks in the mast cell genome.

References

1. Galli, S. J. & Tsai, M. IgE and mast cells in allergic disease. *Nature Medicine* **18**, 693–704 (2012).
2. Bachert, C., Maurer, M., Palomares, O. & Busse, W. W. What is the contribution of IgE to nasal polyposis? *Journal of Allergy and Clinical Immunology* **147**, 1997–2008 (2021).
3. Maurer, M. *et al.* Mast cells drive IgE-mediated disease but might be bystanders in many other inflammatory and neoplastic conditions. *J Allergy Clin Immun* **144**, S19–S30 (2019).
4. Church, M. K., Kolkhir, P., Metz, M. & Maurer, M. The role and relevance of mast cells in urticaria. *Immunol Rev* **282**, 232–247 (2018).
5. Altrichter, S. *et al.* Total IgE as a Marker for Chronic Spontaneous Urticaria. *Allergy Asthma Immunol Res* **13**, 206–218 (2021).
6. Maurer, M. *et al.* Immunoglobulin E-Mediated Autoimmunity. *Frontiers in Immunology* **9**, 689 (2018).
7. McNeil, B. D. *et al.* Identification of a mast cell specific receptor crucial for pseudo-allergic drug reactions. *Nature* **519**, 237–241 (2014).
8. Lansu, K. *et al.* In silico design of novel probes for the atypical opioid receptor MRGPRX2. *Nature chemical biology* **13**, 529–536 (2017).
9. McNeil, B. D. MRGPRX2 and Adverse Drug Reactions. *Front. Immunol.* **12**, 676354 (2021).
10. Komi, D. E. A., Wöhrle, S. & Bielory, L. Mast Cell Biology at Molecular Level: a Comprehensive Review. *Clin Rev Allerg Immu* **58**, 342–365 (2019).
11. Rescigno, M. Intestinal microbiota and its effects on the immune system. *Cellular Microbiology* **16**, 1004–1013 (2014).
12. Tan, J. *et al.* The Role of Short-Chain Fatty Acids in Health and Disease. in vol. 121 91–119 (Elsevier).
13. Koh, A., Vadder, F. D., Kovatcheva-Datchary, P. & Bäckhed, F. From Dietary Fiber to Host Physiology: Short-Chain Fatty Acids as Key Bacterial Metabolites. *Cell* **165**, 1332–1345 (2016).
14. Hee, B. van der & Wells, J. M. Microbial Regulation of Host Physiology by Short-chain Fatty Acids. *Trends Microbiol* **29**, 700–712 (2021).
15. Kespohl, M. *et al.* The Microbial Metabolite Butyrate Induces Expression of Th1-Associated Factors in CD4⁺ T Cells. *Front Immunol* **8**, 1036 (2017).

16. Thio, C. L.-P., Chi, P.-Y., Lai, A. C.-Y. & Chang, Y.-J. Regulation of type 2 innate lymphoid cell–dependent airway hyperreactivity by butyrate. *Journal of Allergy and Clinical Immunology* **142**, 1867–1883.e12 (2018).
17. Chen, L. *et al.* Microbiota Metabolite Butyrate Differentially Regulates Th1 and Th17 Cells' Differentiation and Function in Induction of Colitis. *Inflamm Bowel Dis* **25**, 1450–1461 (2019).
18. Kim, S.-H., Cho, B.-H., Kiyono, H. & Jang, Y.-S. Microbiota-derived butyrate suppresses group 3 innate lymphoid cells in terminal ileal Peyer's patches. *Sci Rep-uk* **7**, 3980 (2017).
19. Sanchez, H. N. *et al.* B cell-intrinsic epigenetic modulation of antibody responses by dietary fiber-derived short-chain fatty acids. *Nat Commun* **11**, 60 (2020).
20. Schulthess, J. *et al.* The Short Chain Fatty Acid Butyrate Imprints an Antimicrobial Program in Macrophages. *Immunity* **50**, 432–445.e7 (2019).
21. Kaisar, M. M. M., Pelgrom, L. R., Ham, A. J. van der, Yazdanbakhsh, M. & Everts, B. Butyrate Conditions Human Dendritic Cells to Prime Type 1 Regulatory T Cells via both Histone Deacetylase Inhibition and G Protein-Coupled Receptor 109A Signaling. *Frontiers in Immunology* **8**, 1429 (2017).
22. Luu, M. *et al.* Regulation of the effector function of CD8⁺ T cells by gut microbiota-derived metabolite butyrate. *Sci Rep-uk* **8**, 14430 (2018).
23. Nastasi, C. *et al.* Butyrate and propionate inhibit antigen-specific CD8⁺ T cell activation by suppressing IL-12 production by antigen-presenting cells. *Sci Rep-uk* **7**, 14516 (2017).
24. Schilderink, R., Verseijden, C. & Jonge, W. J. de. Dietary Inhibitors of Histone Deacetylases in Intestinal Immunity and Homeostasis. *Frontiers in Immunology* **4**, 226 (2013).
25. Chang, P. V., Hao, L., Offermanns, S. & Medzhitov, R. The microbial metabolite butyrate regulates intestinal macrophage function via histone deacetylase inhibition. *Proceedings of the National Academy of Sciences* **111**, 2247–2252 (2014).
26. Creighton, M. P. *et al.* Histone H3K27ac separates active from poised enhancers and predicts developmental state. *Proceedings of the National Academy of Sciences* **107**, 21931–21936 (2010).
27. Zentner, G. E., Tesar, P. J. & Scacheri, P. C. Epigenetic signatures distinguish multiple classes of enhancers with distinct cellular functions. *Genome Res* **21**, 1273–1283 (2011).
28. Whyte, W. *et al.* Master Transcription Factors and Mediator Establish Super-Enhancers at Key Cell Identity Genes. *Cell* **153**, 307–319 (2013).

29. Davie & James, R. Inhibition of Histone Deacetylase Activity by Butyrate. *The Journal of Nutrition* **133**, 2485S-2493S (2003).
30. Licciardi, P., Ververis, Hiong & Karagiannis. Histone deacetylase inhibitors (HDACIs): multitargeted anticancer agents. *Biologics Targets Ther* **Volume 7**, 47 (2013).
31. Eberharter, A. & Becker, P. B. Histone acetylation: a switch between repressive and permissive chromatin. *Embo Rep* **3**, 224–229 (2002).
32. Gallinari, P., Marco, S. D., Jones, P., Pallaoro, M. & Steinkühler, C. HDACs, histone deacetylation and gene transcription: from molecular biology to cancer therapeutics. *Cell Research* **17**, 195–211 (2007).
33. Folkerts, J. *et al.* Butyrate inhibits human mast cell activation via epigenetic regulation of FcεRI-mediated signaling. *Allergy* **75**, 1966–1978 (2020).
34. Bannister, A. J. & Kouzarides, T. Regulation of chromatin by histone modifications. *Cell Res.* **21**, 381–395 (2011).
35. Lovén, J. *et al.* Selective Inhibition of Tumor Oncogenes by Disruption of Super-Enhancers. *Cell* **153**, 320–334 (2013).
36. Zhuang, H.-H., Qu, Q., Teng, X.-Q., Dai, Y.-H. & Qu, J. Superenhancers as master gene regulators and novel therapeutic targets in brain tumors. *Exp. Mol. Med.* **55**, 290–303 (2023).
37. Nguyen, T. *et al.* HDAC inhibitors elicit metabolic reprogramming by targeting super-enhancers in glioblastoma models. *J. Clin. Investig.* **130**, 3699–3716 (2020).
38. Filippakopoulos, P. *et al.* Selective inhibition of BET bromodomains. *Nature* **468**, 1067–1073 (2010).
39. Jiang, G., Deng, W., Liu, Y. & Wang, C. General mechanism of JQ1 in inhibiting various types of cancer. *Mol. Med. Rep.* **21**, 1021–1034 (2020).
40. Bounab, Y. *et al.* Proteomic analysis of the SH2 domain-containing leukocyte protein of 76 kDa (SLP76) interactome in resting and activated primary mast cells [corrected]. *Mol. Cell. Proteom. : MCP* **12**, 2874–89 (2013).
41. Iyer, V. S. *et al.* Modulating T-cell activation with antisense oligonucleotides targeting lymphocyte cytosolic protein 2. *J. Autoimmun.* **131**, 102857 (2022).
42. Saitoh, S. *et al.* LAT is essential for FcεRI-mediated mast cell activation. *Immunity* **12**, 525–535 (2000).
43. Suzuki, R. *et al.* Molecular Editing of Cellular Responses by the High-Affinity Receptor for IgE. *Science* **343**, 1021–1025 (2014).

44. Li, W. & Sun, Z. Mechanism of Action for HDAC Inhibitors—Insights from Omics Approaches. *Int J Mol Sci* **20**, 1616 (2019).
45. Kim, Y. J. *et al.* HDAC inhibitors induce transcriptional repression of high copy number genes in breast cancer through elongation blockade. *Oncogene* **32**, 2828–2835 (2013).
46. Greer, C. B. *et al.* Histone Deacetylases Positively Regulate Transcription through the Elongation Machinery. *Cell Reports* **13**, 1444–1455 (2015).
47. MacDonald, C. A., Qian, H., Pundir, P. & Kulka, M. Sodium butyrate suppresses malignant human mast cell proliferation, downregulates expression of KIT and promotes differentiation. *Front. Allergy* **4**, 1109717 (2023).
48. Wang, Z. *et al.* Genome-wide Mapping of HATs and HDACs Reveals Distinct Functions in Active and Inactive Genes. *Cell* **138**, 1019–1031 (2009).
49. Rada-Iglesias, A. *et al.* Butyrate mediates decrease of histone acetylation centered on transcription start sites and down-regulation of associated genes. *Genome Res* **17**, 708–719 (2007).
50. Sanchez, G. J. *et al.* Genome-wide dose-dependent inhibition of histone deacetylases studies reveal their roles in enhancer remodeling and suppression of oncogenic super-enhancers. *Nucleic Acids Res* **46**, 1756–1776 (2017).
51. Gryder, B. E. *et al.* Chemical genomics reveals histone deacetylases are required for core regulatory transcription. *Nature Communications* **10**, 3004 (2019).
52. Cildir, G. *et al.* Genome-wide Analyses of Chromatin State in Human Mast Cells Reveal Molecular Drivers and Mediators of Allergic and Inflammatory Diseases. *Immunity* **51**, 949–965.e6 (2019).
53. Heinz, S. *et al.* Simple Combinations of Lineage-Determining Transcription Factors Prime cis-Regulatory Elements Required for Macrophage and B Cell Identities. *Molecular Cell* **38**, 576–589 (2010).
54. Zhou, Y. *et al.* Metascape provides a biologist-oriented resource for the analysis of systems-level datasets. *Nat Commun* **10**, 1523 (2019).
55. Stadhouders, R. *et al.* Epigenome analysis links gene regulatory elements in group 2 innate lymphocytes to asthma susceptibility. *J Allergy Clin Immun* **142**, 1793–1807 (2018).
56. Kim, D., Langmead, B. & Salzberg, S. L. HISAT: a fast spliced aligner with low memory requirements. *Nature Methods* **12**, 357–360 (2015).
57. Kuehn, H. S., Radinger, M. & Gilfillan, A. M. Measuring Mast Cell Mediator Release. *Curr Protoc Immunol* **91**, 7.38.1–7.38.9 (2010).